OPGW Corrosion Detection Using Nondestructive Test Method

Jae-Kee Jeong, Gi-Gab Yoon, Ji-Won Kang and Hai-Won Yang

Abstract

This paper deals with some characteristics of a nondestructive eddy current detector to measure OPGW(composite overhead ground wire with optical fiber) corrosion. This detector is designed to automatically run on OPGW and to continuously inspect the corrosion of the line. The impedance of the eddy current coil changing by any corrosion phenomenon of OPGW is analyzed. Several performances of the detector are described and experimental procedures and test results are also given. As a result, it is shown that the implemented detector can be measured some quantitative data for crack, broken wires or severe deteriorations in OPGW. This nondestructive test method would be applied to improve the reliability and efficiency of transmission lines in service.

I. Introduction

Power transmission lines generally consist of two parts. One is the power lines which mainly play the important role of transmitting electric power. The other is the ground wires to protect power lines from the lightning strokes and sometimes to use as fault current paths. Conventionally ACSR(Aluminum Conductors Steel Reinforced) has been used as the ground wire, but in recent it would be more common to adapt OPGW as the same function. Such an OPGW has optical fibers in the center of wire. The optical fibers are used to communication lines which can make phone call and communicate various informations about operating and diagnosing power equipments. Therefore, the OPGW would be helpful to provide high quality electric power to consumers.

OPGW is composed of two layers. In center there is a aluminum tube which keeps the fiber from steep vending and losing its function. The outer layer is strands of aluminum clad steel wire to endure tensional strength and to make use of fault current paths.

OPGW installed at marine area and industrial area exposures under any full condition for easy to corrode aluminum. After corroded aluminum clad, the steel core appears in air, and then the atmospheric corrosion of OPGW

would be speed up. At last strands would be cut off[1~2].

In this paper we deals with corrosion detection using a detector which automatically runs on a OPGW line and inspects the corrosion of the conductor by utilization of the nondestructive eddy current test with respect to the artificial corrosions. At first theoretical basis is introduced. And then specifications of detector, test procedures and test results are described.

II. Characteristics of Eddy Current Sensor

Figure.1 shows a solenoid coil with a conductive material. When an alternating sinusoidal input is applied to the sensor coil, the magnetic flux determined by the coil turns and input current is generated. If the test material is inserted inside the sensor, the total magnetic flux is changed by the electromagnetic property and structure of the material[3-4]. The main magnetic flux affects the eddy current generated on the test conductor. Therefore the sensor impedance would be
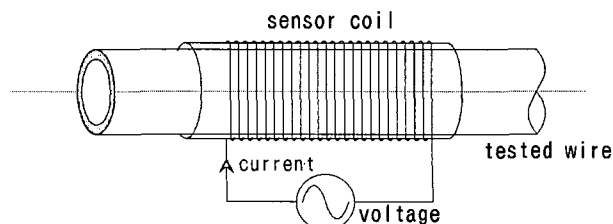

Fig. 1. Solenoid coil sensor and test material.

changed by the electromagnetic and geometric aspects to the material. Those properties, then, can be detected and quantified using a proper measuring method.

First, consider the air-cored sensor without any test material. When constant alternating current, $i(t) = I_m e^{j\omega t}$, is applied to the sensor, the internal magnetic field intensity of the sensor, $h_0(t)$[AT/m] becomes to be uniform and is expressed as the following equation.

$$h_o(t) = n i(t) = H_o e^{j\omega t} \tag{1}$$

where $n = N/\ell$ is the coil turns per unit coil length ℓ [m], and N denotes the coil turns. In this case, the magnetic flux density in air-cored coil, $b_o(t)$[Wb/m^2], becomes

$$b_o(t) = \mu_o H_o e^{j\omega t} \tag{2}$$

where μ_o is the magnetic permeability of air space, i. e., $\mu_o = 4\pi \times 10^{-7}$ [H/m]. Consequently, the magnetic flux inside the air-cored coil ϕ_o [Wb] can be described as follows

$$\phi_o(t) = \Phi_o e^{j\omega t} \tag{3}$$

where $\Phi_o = \mu_o H_o A_o = B_o A_o$. $A_0 = \pi r_0^2$ is the cross section area of coil and r_0[m] is the mean radius of bobbin.

Because of the magnetic flux linkage with solenoid coil, the voltage across the sensor coil is given by

$$\begin{aligned} v_o(t) &= Ri(t) + N\frac{d\phi_o(t)}{dt} \\ &= (R + j\omega\mu_o n^2 \ell A_o)I_m e^{j\omega t} \end{aligned} \tag{4}$$

Assuming that the coil resistance is negligible in Eq. (4), the air-cored coil impedance, $\dot{Z}_o$, can be written as

$$\dot{Z}_o = j\omega\mu_o n^2 \ell A_o = j\omega L_o \tag{5}$$

where $L_o = \mu_o n^2 \ell A_o$ [H]. From Eqs. (4) and (5), we can easily know that the sensor impedance is proportional to the magnetic flux linkage with the coil.

On the other hand, inserting a test material into the sensor, the eddy current generated ion the conductor is induced by the magnetic field intensity.

$$\text{curl } H = J \tag{6}$$

where J[A/m^2] and H[AT/m] denote the current density and the magnetic field intensity, respectively. The internal magnetic flux and the eddy current density of the conductor is given by $B = \mu_r H$ and $J = \sigma E$, respectively, where $\mu = \mu_0\mu_r$ denotes the permeability of the material and E[V/m] is the electrical field intensity.

The magnetic flux density, $b(t)$, of the test material can be obtained using simple electromagnetic performance, and is expressed as the following equation

$$\nabla^2 b(t) = \mu\sigma\frac{db(t)}{dt} \tag{7}$$

As the direction of the magnetic field and flux density are coaxial with coil, only the z-axis component of magnetic flux would be considered. Thus, the flux density of Eq. (7) can be written as follows.

$$b(t) = kBe^{j(\omega t + \theta)} \tag{8}$$

where $B = \mu_r B_o$ and the amplitude and phase, k and θ are given by

$$k = e^{-\alpha}, \quad \theta = -\alpha \tag{9}$$

In this equation, $\alpha = z/\delta$ denotes the amplitude attenuation ratio and the standard depth of penetration, δ, is defined as.

$$\delta = \sqrt{\frac{2}{\omega\mu_o\mu_r\sigma}} \tag{10}$$

Consequently, the magnetic flux penetrated into the test material would be changed by the relative magnetic permeability, electrical conductivity of the test material and source frequency. And the magnetic flux has an exponential attenuation property as permeating the center of conductor. When $z = \delta$, this Eq. (9) describes the standard depth of penetration at which the eddy current density has been reduced to 37[%] of its value on the surface. It is also known in Eq. (8) that the phase of B is delayed by $-z/\delta$ in accordance with the magnetic flux density of the conductor surface. From these Eqs. (8) and (9), the eddy current and the total flux of the coil are varied by electric quantities and source frequence. Therefore, it is easily expected that the impedance of sensor coil would be also changed.

Since the strands of aluminum clad steel wire in the outer layer of OPGW consists of 2 different metals, the standard penetration depth for 2 metals and the effect of eddy current would appear as complex phenomenon.

For the purpose of analysis, consider the test materials, M1 and M2 of the air-cored coil with the relative magnetic permeability, μ_1, μ_2 and the electrical conductivity, σ_1, σ_1, respectively. Since the magnetic flux density of the air gap is B_o, the surface magnetic flux density of M_1 becomes to be $B_{1a} = \mu_1 B_o$. Then, penetration flux on the surface of M_1 is decreased, in accordance with Eqs. (8), (9) and (10). The magnetic flux density on the surface of M_2, thus, is given as

$$B_{1b} = \mu_1 B_o e^{-d_1/\delta_1} \tag{11}$$

where δ_1 indicates the standard depth of penetration determined on M_1.

Since the magnetic flux density on the surface of aluminum clad steel wire is given as $B_{2a} = \mu_2 B_{1b}$, the magnetic flux through M_2 would be changed by the metallic performance of M_2. In this case, the magnetic flux density is decreased as much as going into the inner side and the magnetic flux of M_2 at the center can be described as follows
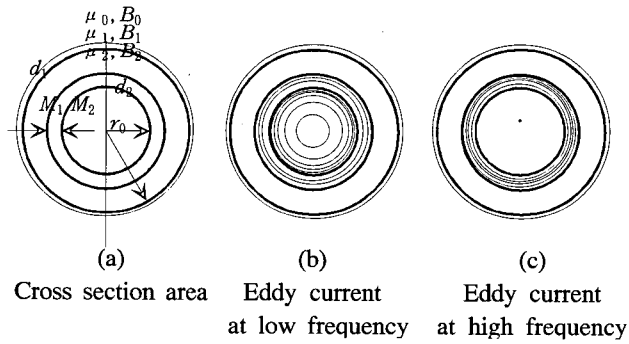
(a)　　　　　　(b)　　　　　　(c)

Cross section area　Eddy current　Eddy current
　　　　　　　at low frequency　at high frequency

Fig. 2. Simulation results of an aluminum claded steel wire.

$$B_{2b} = B_{2a}e^{-d_2/\delta_2} \qquad (12)$$
$$= \mu_1 \mu_2 B_o e^{-\left(\frac{d_1}{\delta_1} + \frac{d_2}{\delta_2}\right)}$$

For the aluminum clad steel wire, the distribution of the flux density is estimated to Fig. 2 (b) and (c).

It may not be easy to quantify with the magnitude or phase variation. Therefore, in this study, only the magnitude of impedance is considered to detect the quantity for aluminum coating adherence and coating state. Letting $\Delta \dot{Z}$ be the impedance change by the material, we can obtain by the following equation[5].

$$\Delta \dot{Z} = \{a_1 + j(a_2 - 1)\}\eta \omega L_o \qquad (13)$$

where η is the fill factor and a_1 and a_2 are related to the excited frequency

If the exciting frequency increase from '0' to '∞', the normalized reactance trajectory starts at $1 + (\mu_r - 1)\eta$, and ends at $1 - \eta$ as the frequency increases to infinity. Consequently, it is easily known that the cross section area of the test material can be detected from the impedance variation at a high frequency. In general, the impedance change due to the zinc loss in the galvanized steel core of OPGW, appears obviously at tens of kHz.

III. Corrosion detector design

A corrosion detector system to run automatically on the OPGW was developed under having the following five objectives.
- Design of eddy current sensor and its theoretical analysis
- Nondestructive corrosion inspection by the detector with eddy current sensor
- On-line data acquisition of corrosion state and test length while running it along the line
- Capability to change the frequency range, current amplitude and motor speed.
- Setting the frequency and amplitude of current source

and operating the driving motor by a portable computer.

Under the assumptions described above, a nondestructive corrosion detector was designed as shown Fig.3. To excite a solenoid coil, a constant current source with variable frequencies was implemented and the output of the sensor is converted using 16-bit AD converter. The measurement data can be acquisited to the memory with on-line.
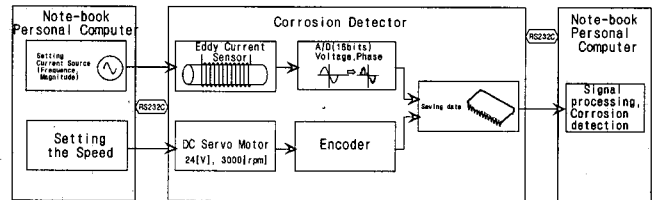

Fig. 3. Block diagram of detector for testing.

On the other hand, a servo motor control system was also designed which has the capabilities such as speed control and distance measurement. Moreover, such operations as setting an operational frequency, adjusting a suitable current amplitude or analyzing corrosion state can be performed by using a personal computer. Then, some important specifications for the designed corrosion detector are described in Table 1.

Table 1. Specifications of the developed corrosion detector.

Items	Specifications
Size	400×550×190[mm]
Weight	26[kg]
Figure of Coil	Normal Single Layer ECT Coil
Running Speed	0 - 13[m/min]
Control Source	Battery
Power Source	Frequency-Variable Current Source
Data Acquisition	Impedance(Amplitude, Phase), Running Interval
Number of Data Acquisition	Over 30,000 data
Communication to Computer	RS-232C Serial Port
Control Method	Control using Wire Radio(Moving Forward, Backward, Stop)
Operating	Impossible
Safety Device	Non-use

IV. Test and Measurements

The measurement results and method using the device are

explained in this section.

Test was performed at the place that constructed to be able to be efficient test. The results would aimed at nondestructive test of transmission line after establishing the relationship between mechanical characteristics and this test results .

1. Test facilities

Fig.4 shows the test place and devices to install an OPGW at a .field. The followings are basic specifications of the testing system.
- Total length of span : 35[m]
- Support wires to endure tensions
- Capability to adjust the dip and slope of the test OPGW by winches and pulleys
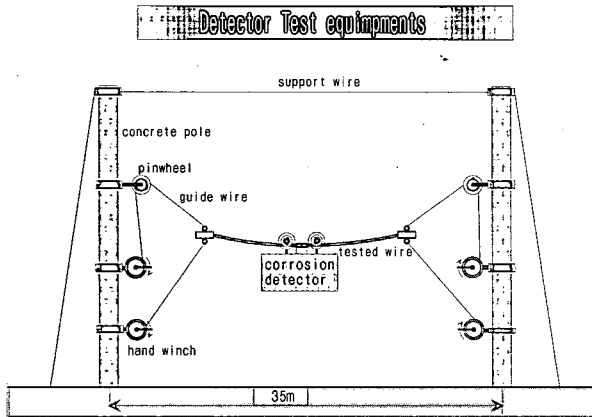- Subsystems to easily pull the detector and the line up and down

Fig. 4. Test Yard.

2. Test schedule

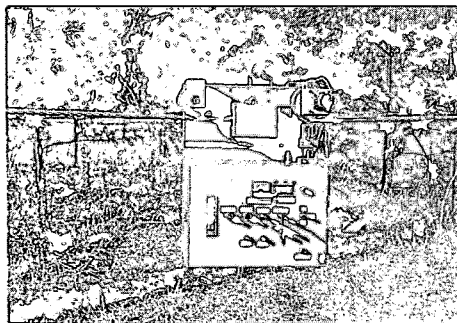Fig 5 shows the designed corrosion detector running on the OPGW.

Fig. 5. Running and inspecting feature of the developed corrosion detector.

Operating and testing process of the corrosion detector are described as follows.

1) Set up speed limit of the servo motor, test length, numbers of data acquisition at each measuring point, the amplitude and frequency of current source using a potable computer and measurement devices.

2) Remove the RS232C cable from the detector and the potable computer.

3) If the corrosion detector is started by pushing button, it would accept running interval, measuring data as well stop operation at a position chosen by the test distance.

4) Connecting communication cable again, corrosion data could be read into the portable computer

5) Process 1) - 4) is repeated with varying amplitude and frequency of the current source until obtained any satisfied data.

6) After acquisiting the measured data, the test wires are removed from the measuring system to analyze the degree of corrosion and to test mechanical strength in the laboratory.

7) Finally, the relationship between corrosion degrees and mechanical characteristics is examined by a proper analyzing program.

3. Validation for application

To test and verify the efficiency of the designed corrosion detector, an OPGW, 100[mm^2] was used as a test material. Fig 6 illustrates the cross section feature of the OPGW sample. Since theoretical results obtained in Sec. 2 is for a single rod and pure metallic component material, all strands area in Fig. 6(a) is assumed to be an equivalent one as shown in Fig. 6(b).

As the conductivity and permeability of aluminum is 61[%] and $\mu_r = 1$, respectively, and the wall thickness of aluminum clad is 0.431[mm], the frequency corresponding that the standard penetration depth would be equal to the thickness, becomes to be about 39[kHz]. This calculation result coincides with the test frequency explained in Sec. 4.4 with reference to the corrosion detector. From the view of this, it is possible to estimate that the equivalent outer depth of aluminum would be 0.431[mm].
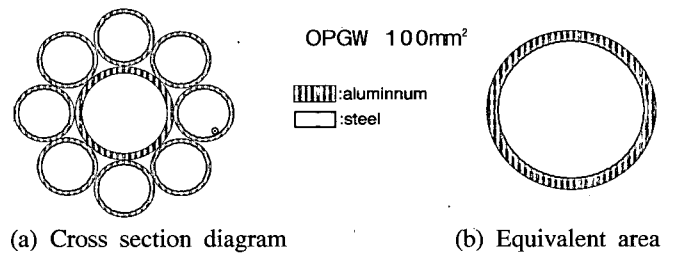

(a) Cross section diagram   (b) Equivalent area

Fig. 6. OPGW under testing.

4. Test results and observation

To examine the developed corrosion detector, an OPGW corroded in chrolide resolution, was prepared. Fig 7(a) shows

the detector outputs from 1kHz to 35kHz in the relatively low frequency range which penetrates the aluminum depth. As you can see in Fig 7(a), there were normal ferromagnetic eddy current characteristics that only the steel wire is reacted.

It was one very important fact that the effect of the clad aluminum thickness was to screen the underlying steel from the applied field so that the response of the steel wire shows a high or low level in accordance with the degree of aluminum thickness. In other words, the eddy current by the thickness of the aluminum clad prevented the magnetic flux to go into steel inside.

In this point, we could know that it was possible to predict the corrosion degree of the aluminium clad through the response degrees of the steels.
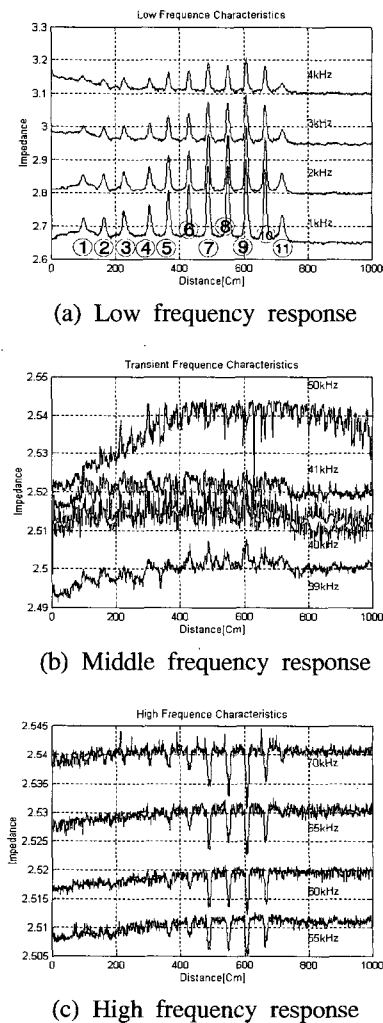

(a) Low frequency response

(b) Middle frequency response

(c) High frequency response

Fig. 7. Outputs of the corrosion detector.

The detect outputs for the middle frequency range, 35[kHz] to 50[kHz], is shown in Fig. 7(b). In this frequency range, there exist some disorders, because both steel and aluminum clad would be reacted to outer field. Therefore, it was not easy for the output signals to distinguish any reaction performance of the steel or aluminum. So we should select this frequency range in order to inspect the OPGW.

Fig. 7(c) shows the detector outputs for relatively high frequency range above 55[kHz]. In this frequency range, it was also impossible for the outer magnetic field to go into steel inside. However, it may be guess that the impedance output is revealed any normal non- ferromagnetic characteristics for the aluminum clad.

Fig. 8 shows the cross section area of the corroded parts, after testing OPGW was removed from the span. The each number below the pictures of Fig. 8 corresponds to that of Fig. 7(a). And the number 13 is no corrosion part. But it is impossible to discriminate with naked eyes whether any part is corroded or not. In order to clarify this point, Figure 3 is tried. Figure 3 illustrates that the comparison between the normal strand and the corroded strand labeled ④ in Fig. 8 . As shown in Fig. 9, the width of the most thin part is 0.258[mm] which is about 60% compared to that of normal strand.
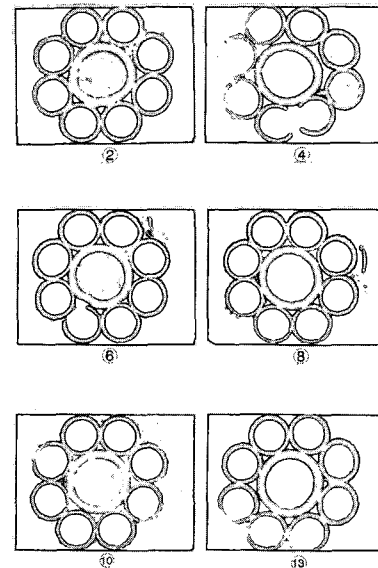

Fig. 8. Cross section pictures for corrosion parts for the artificial cracked OPGW.
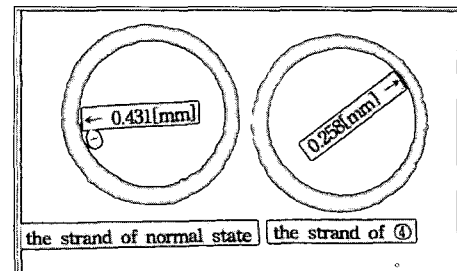

Fig. 9. Comparision of a normal strand with the corroded strand.

In this connection we can make a very important conclusion that it is possible to distinguish which material part, steel or aluminum corrodes and to detect how much degrees of each part are in OPGW. Here we can induce the rule to know which corrosions are as shown in Table 2.

Table 2. Corrosion decisions.

low frequencies	high frequencies	corrosion decisions
O	O	Al or Steel
O	O	Al
O	O	No corrosion
O: response	O: non-response	

V. Conclusion

The nondestructive corrosion detector, running on an OPGW and inspecting the line with on-line is developed in this research. Several properties for eddy current sensor such as the normalized impedance, standard penetration depth of magnetic flux and impedance variation by electromagnetic and geometrical aspects are also discussed.
It is shown that the implemented detector is possible with reliable to inspect the corrosion of OPGW, through testing and experimental studying for artificial corroded samples. As

the result, a new rule for deciding corrosion states is suggested and the aluminum partial corrosion is efficiently detected with according to the rule. It may be very useful to detect the corrosion of such an OPGW by using this kind of detector. Futhermore, we believe that this technique would be applied to diagnose other transmission and distribution lines.

References

[1] J. Blitz, Electrical and Magnetic Methods of Nondestructive Testing, Adam Hilger, pp.91~103, 1991.
[2] J. Blitz, "Prediction of impedance components of eddy current coil using a PC", NDT International, Vol.22, No.1, pp.3~6, 1990.
[3] F. Thollon, B. Lebrun, N. Burais and Y. Jayet, "Numerical and experimental study of eddy current probes in NDT of structures with deep flaws", NDT International, Vol.28, No.2, pp.97~102, 1995.
[4] Z. Molttl, "The quantitative relations between true and standard depth of penetration for air-cored probe coils in eddy current testing", NDT International, Vol.23, No.1, pp.11~18, 1990.
[5] JK, Jeong, HW, Yang, "Eddy Current Sensor to detect Zinc Loss of Galvanized Steel Wires", KIEE Trans., Vol. 45, pp. 1033~1038, No. 7, JUL. 1996.
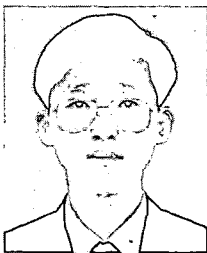
Jae-Kee Jeong was born in Chung-Buk, Korea. He received the B.S. degree in Electrical Engineering from Chung-Nam University in 1985 and M.S. and Ph. D. degree in Electrical Engineering from Han-Yang University in 1987, 1997, respectively. He is Senior Member of Technical Staff in KEPRI. His research interests are diagonoses for power equipments.
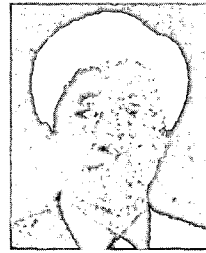

Ji-Won Kang was born in Pusan Korea. He received the B.S. and M.S. degree in Electrical Engineering from Han-Yang University in 1987, 1993, respectively. He is working for Ph. D degree in Electrical Engineering from Han-Yang University and is Senior Member of Technical Staff in KEPRI. His research interests are power system control.

Gi-Gab Yoon was born in Chung-Buk, Korea. He received the B.S. and M.S. degree in Electrical Engineering from Han-Yang University in 1983, 1988, respectively. He is working for Ph. D degree in Electrical Engineering from Han-Yang University and is Junior Member of Technical Staff in KEPRI. His research interests are power system control.

Hai-Won Yang was born in Seoul Korea. He received the B.S. and M.S degree in Electrical Engineering Seoul National University in 1971, 1973, respectively and Ph. D. degree in Electrical Engineering from Kyoto University, Japan in 1982. He started from associated professor at Myung-Gi University. He has served as a professor in the Department of Electrical Engineering at Hang-Yang University since 1986. His current research interests are adaptive control for nonlinear system using neural networks and power system control.